FMDB *Transactions on Sustainable Structures and Materials*

Mitigating Explosive Thermal Spalling in RPC with Polypropylene Fibers: Structural Mechanisms and AI-Driven Modeling

Mohammed K. Abed[1], Isam M. Ali[2,*], Mohammed Salah Nasr[3], Ahmed Samir Naje[4], Anishbhai Vahora[5], Abul Hasan[6]

[1,2]Department of Civil Techniques, Al-Furat Al-Awsat Technical University, Kufa, Al-Najaf, Iraq.
[3]College of Engineering, University of Babylon, Hillah, Babylon, Iraq.
[4]Department of Water Resources Engineering Management, College of Engineering, Al-Qasim Green University, Al-Qasim, Babylon, Iraq.
[5]Department of Engineering, Brask Inc. – IEE, Sulphur, Louisiana, United States of America.
[6]Department of Mechanical Engineering Technology, Augusta Tech Drive, Augusta Technical College, Augusta, Georgia, United States of America.
mohammed-k1965@atu.edu.iq[1], inkr.asm@atu.edu.iq[2], eng511.mohammed.nasr@uobabylon.edu.iq[3], ahmed.sameer@wrec.uoqasim.edu.iq[4], avahora@ieeinc.net[5], abul.hasan@augustatech.edu[6]

Abstract: This research investigates the overall mechanical and thermal performance of reactive powder concrete (RPC) subjected to elevated temperatures of 250°C, 400°C, and 600°C for soaking periods of 30 and 60 minutes. Two mixture designs were evaluated: a conventional reference matrix (Mix R) with a low water-binding ratio of 18%, and a fibre-reinforced composite containing 0.2% volume fraction of polypropylene (PP) fibres (Mix RF). Each mixture was hyperthermally stable at 250°C, with internal autoclaving favouring secondary pozzolanic reactions. Compressive losses were 2.50% for Mix R and 3.49% for Mix RF at 28 days. At 400°C, portlandite and calcium-silicate hydrate (C-S-H) gel dehydrated, decreasing compressive strength by 14.5% and 17.1%, respectively. This effect intensified after 60 minutes of soaking. The traditional matrix (Mix R) at 600°C had destructive, explosive thermal spalling and premature failure due to asymmetric internal vapour flow trapped in its ultradense microstructure. However, adding 0.2% PP fibres to Mix RF melted them, creating a continuous network of interconnected microcapillary channels that efficiently facilitated internal hydrostatic vapour flow, maintaining structural integrity and providing a controlled, progressive thermal degradation pathway for internal vapour-stress relief. By providing micro-channels for internal vapour pressure relief, 0.2% polypropylene fibres prevent explosive thermal spalling in Reactive Powder Concrete (RPC) at 600°C. The AI model also accurately predicted residual compressive strength (R2 = 0.999), suggesting that fibre dose is the most important element with a 50.2% relative contribution.

Keywords: Reactive Powder Concrete (RPC); Thermal Degradation; Elevated Temperature; Thermal Spalling; Hyperthermal Stability; Compressive Strength; Microcapillary Channels.

Received on: 23/06/2025, **Revised on:** 08/10/2025, **Accepted on:** 19/10/2025, **Published on:** 05/06/2026

Journal Homepage: https://www.fmdbpub.com/user/journals/details/FTSSM

DOI: https://doi.org/10.69888/FTSSM.2026.000757

Cite as: M. K. Abed, I. M. Ali, M. S. Nasr, A. S. Naje, A. Vahora, and A. Hasan, "Mitigating Explosive Thermal Spalling in RPC with Polypropylene Fibers: Structural Mechanisms and AI-Driven Modeling," *FMDB Transactions on Sustainable Structures and Materials*, vol. 2, no. 1, pp. 52–69, 2026.

[*]Corresponding author.

1. Introduction

Reactive powder concrete (RPC) represents a significant advancement in cementitious materials, characterised by very high compressive strength, good durability, and a very dense microstructure compared to conventional concrete [1]; [2]. Despite their exceptional mechanical properties, the behaviour of RPC under high-temperature environments remains a critical structural issue [3]. Because of its ultra-low permeability and extremely dense particle packing, internal moisture within the matrix cannot be readily removed when exposed to fire or extreme temperatures. This physical barrier traps high-pressure water vapour within micropores, rapidly raising internal vapour pressure to match external pressure. This may threaten the structural integrity of concrete aggregates [4]; [7]. To reduce the inherent weaknesses, extensive traditional and current studies have focused on the thermal, chemical and mechanical transformations of this superior material. The initial studies described the fundamental hazards and degradation mechanisms governing concrete structures during thermal ageing. Noumowe et al. [5] confirmed that innovative heating causes sharp changes in internal porosity, with elevated vapour flow tightly coupled to permeability transitions. Sultan and Alyaseri [6] evaluated the effect of increasing temperature from 200°C to 500°C. The findings showed a transient, proportional decrease in residual strength with increasing temperature and propagation time. In addition, higher cement content, which increases the initial ambient energy, increases the rate of overall performance loss during put-up promotion. At the same time, incorporating metallic fibres helps maintain integrity up to 150°C.

Researchers have also extensively studied the effects of the proportion of immature fabric and contour changes in the low-to-moderate temperature regime. However, when heat promotion is pushed to excessive levels, Canbaz [3] found that heating RPC to 900°C for 3 hours causes profound physicochemical degradation, leading to severe microstructural collapse, extensive cracking, and structural damage. In the current decade, RPC research has shifted toward high-resolution microstructural modelling and revolutionary spalling-mitigation techniques. Chadli et al. [8] investigated delicate fractures in an ultra-dense cementitious matrix and showed that microstructural relaxation and chemical destabilisation begin simultaneously before the observed macrocracks appear. Mao et al. [9] investigated the role of polypropylene (PP) fibres in preventing explosive failure, showing that melting fibres form continuous microcapillary channels that draw out internal vapour pressure in a hybrid matrix approach. Abbas et al. [10] reached similar results. In addition, Ashteyat et al. [11] provided a comprehensive framework describing the performance of ultra-high-performance concrete under standard fire curves, while Kanagaraj et al. [12] evaluated the set fire residual load capacity of full-scale RPC columns for specified structural protection. Driven by global sustainability models, the existing literature has focused on green binders and better experimental conditions. Rajkumar et al. [13] thoroughly developed untested RPC mixtures using industrial by-products. They mapped their corresponding thermal responses, and Zhang et al. [14] focused on the comparative dynamics of blast spalling between simple and fibre-reinforced hyperperformance matrices.

At a more detailed level, Cheng et al. [15] evaluated the performance of RPCs fabricated from locally sourced materials under extreme thermal gradients to capture cyclic fatigue. Further, Abid et al. [16] analysed the effects of repetitive thermal cycling on the residual and flexural evolution of RPC, while Ntimugura et al. [17] monitored the microchemical degradation of calcium silicate hydrate (C-S-H) gels up to 800°C using advanced spectroscopic methods. In addition, Yu et al. [18] numerically inferred internal pore-tension dynamics as a function of temperature, linking these fields directly to spalling boundaries. Sultangaliyeva et al. [19] optimised PP fibre expansion fracture, with a perfect boundary configuration, stable explosive spalling immunity and compromised environmental mechanical metrics. Regarding tensile vulnerability, Yu et al. [20] documented the high sensitivity of tensile energy distribution to the temperature gradient, consistent with observations by Hiremath and Yaragal [21]. On the macromechanical degradation of UHPC under extended wetting barriers, Mao et al. [22] evaluated how early hardening schedules affect subsequent fire resistance, while Lucio-Martin et al. [23] mapped microcrack networks generated using incoherent thermal expansion between a combination of debris and a draped binder paste. To capture the physiological variables, Farhangi et al. [24] tuned thermal conductivity and mass loss in dense powder matrices using ascending-temperature barriers. More recently, Ren et al. [25] used Artificial Intelligence (AI) to create predictive mathematical models to calculate the residual potential of RPC after fire events. In a structural language forum, Regalla and Kumar [26] included pilot tests and a detailed final analysis to capture the fire performance of RPC beams, while Tai et al. [27] built on these improvements by introducing nanomaterials to enhance the thermal stability of cementitious matrices under ultra-high temperatures.

These contemporary insights are strongly consistent with older data; for example, Paiva et al. [28] evaluated the evolution of residual peak pressure in metal fibre-reinforced RPC up to 500°C. They showed that ternary pozzolanic mixtures (silica fume, slag, and fly ash) undergo excessive microstructural degradation near 1000°C. Locally, Abdul-Rahman et al. [30] observed that adding polyvinyl chloride fibres reduced spalling at 600°C, despite the surprising reduction in hardness. Importantly, Kubba et al. [31] noted that PP fibre could help concrete withstand high-temperature exposure. A current outlook addresses an important research gap by systematically investigating the overall structural performance of RPC under focused temperatures (250°C, 400°C, and 600°C) with specific soaking times of 30 and 60 min. It clearly assesses compressive, splitting tensile and flexural strength failure and describes how 0.2% polypropylene fibres prevent catastrophic explosive spalling and maintain structural flexibility under extreme fire stress [7]. Recently, the incorporation of Artificial Intelligence (AI) and machine learning (ML)

techniques has enabled the development of a powerful model to evaluate and predict the complex thermo-mechanical behaviour of advanced cementitious composites [32]. Applying AI-driven predictive models allows researchers to accurately forecast residual mechanical strengths (compressive, splitting tensile, and flexural) and optimise polypropylene fibre dosages [29]. Such computational frameworks not only bridge the gap between experimental observations and theoretical simulations but also significantly enhance the reliability, efficiency, and forward-looking scientific firmness of modern concrete research [35].

2. Materials

RPC was prepared using commercially available cement. The cement blend was formulated specifically to have low C_3A and high C_3S and C_2S content. Ordinary Portland cement (Type 1) was used in this research work.

Table 1: Chemical composition of cement

Oxide	Content %	Iraqi Specifications (No.5/2019)
SiO_2	22.6	
CaO	62.3	
Al_2O_3	3.1	
Fe_2O_3	3.52	
MgO	2.73	< 5
SO_3	1.25	< 2.5
Free lime	2.64	
L.O.I	0.042	< 4
L.S.F	0.87	0.66-1.02
Insoluble Residue I.R	1.03	< 1.5
C_3S	41.63	
C_2S	28.51	
C_3A	2.27	
C_4AF	10.7	

Its chemical and physical properties met Iraqi specification limits [I.Q.S NO.5/2019], as shown in Table 1 and Table 2, respectively. Highly reactive silica pozzolan is an essential component of RPC, improving composite matrix density and reducing the potential for particle-to-particle voids.

Table 2: Physical properties of cement

Property	Value	Iraqi Specifications (No.5/1984)
Specific Gravity	3.15	
Fineness, Blaine, cm^2/gm	3516	≥ 2300
Setting Time		
Initial: Minutes	138	≥ 45 min.
Final: Hours	4.30	< 10 hr.
Compressive Strength, MPa		
3 days	19.4	> 15
7 days	27.8	> 23

Silica fumes can have very high strength and durability. It has a very large surface area, which improves the concrete microstructure, permeability, crack resistance, and workability [33].

Table 3: Properties of silica fume

Property	Result
Fineness (Blaine)	1570 m^2/g
SiO_2	86.3%
Unit Weight	2.3 g/cm^3
Activity Index	114 %
Chloride Content	< 0.1%

The properties of silica fume are shown in Table 3. Fine aggregate: natural sand used in all concrete mixes with a grading between 0.150 and 0.600 mm. Its grading and sulfate content conform to the Iraqi specification [I.Q.S. No. 45/1984].

Table 4: Grading of fine aggregate (Sand)

Sieve Size (mm)	Passing %
0.6	100
0.3	87
0.15	52
0.075	1

Table 4 shows the grading of the fine aggregate used. High-range water-reducing (HRWR) admixture Gilinume 51 was used to increase the workability of concrete mixes without additional water.

Table 5: Properties of PP fibres

Property	Result
Colour	White
Melting Point	170 ºC
Thermal conductivity ($\times 10^{-4}$ cal/cm-sec- ºC)	2.5-3
Specific Gravity	0.93

The properties of polypropylene fibres (PP) used in this study are shown in Table 5.

2.1. Mix Proportion

Table 6 illustrates the mix proportions of RPC mixes. The table summarises and quantifies the typical mixing ratios optimised for preparing reactive powder concrete (RPC) specimens. Three complete binders at 1080 kg/m3 were used to obtain an ultra-high-strength matrix with an exceptionally dense particle packing.

Table 6: Mix proportions of RPC

Constituent	Weight
Cement kg/m^3	850
Silica fume kg/m^3	230
Fine aggregate (sand) kg/m^3	1100
Polypropylene fibre %	0.2
Superplasticiser by weight of binder %	2.75
Water kg/m^3	195
Water/Binder ratio	0.18

This binder contains 850 kg/m^3 of ordinary Portland cement supplemented with 230 kg/m^3 of ultra-fine silica fume, for a full mass exchange. The incorporation of silica fume into this improved ratio is important for maximising the second pozzolanic reaction by reworking the structurally weak, thermally unstable crystalline portlandite (Ca(OH)2) into high-density calcium-silicate-hydrate (C-S-H) gels.

2.2. Sample preparation

The preparation of the sample elaboration comprises many steps:

- The control mixture was designed with a concrete resistance of 110 MPa at 28 days.
- One hundred and sixty-eight concrete (cube, cylinder, and prism) specimens of (50*50*50) mm^3, (100*200) mm, and (400*100*100) mm, respectively, were cast from each mix.
- After casting, concrete specimens were cured in the water tank.
- After curing, the concrete samples were heated in an electric furnace to temperatures of (250, 400, and 600) ºC for (30 and 60) minutes.

3. Experimental Work

Using an electric furnace with a 1000 ºC capacity, at a heating rate of 15 ºC/minute, specimens were heated to three target temperatures (250, 400 and 600 ºC) for 30 and 60 minutes each. A controlled heating program was conducted to evaluate the residual mechanical performance and thermal equilibrium of reactive powder concrete (RPC) under manifold thermal-mass heat contact. Researchers used a commercial-grade electric muffle furnace with a maximum operating temperature of 1000 °C. Researchers used a constant heating rate of 15 ºC/min to heat from ambient temperature (20±2 ºC) to the set temperatures until the threshold limits were reached. The test matrix included three apparent threshold temperatures: 250 °C, 400 °C, and 600 °C. These characteristic temperature differences correspond to crucial microstructural phases in cementitious composites, specifically: free moisture evaporation, polymer fibre bridge formation and decomposition (250 °C), internal vapour tension peak (400 °C), and early calcium-silicate-dihydrate (600 °C), as reported in the literature. To examine the effect of temperature saturation length on the other tests, samples at each target temperature were held in a static state (soaking length) for 2 soaking periods: 30 minutes and 60 minutes.

After completion of the corresponding soaking periods, the furnace was shut down, and the specimens were allowed to cool completely to room temperature before the next countermechanical test. After 28 days of curing, the specimens were removed from the curing tank and oven-dried for 24 hours to prevent concrete spalling before being subjected to elevated temperatures; they were then exposed to 3 temperatures (250, 400, and 600 °C). For rapid heating, the muffle furnace was modified to ramp up by 15 °C/min until the required temperature was reached. The samples were then kept at the target temperature for 30 or 60 min to ensure thermal equilibrium. After each ramp to the target temperature, the samples were cooled to room temperature and stored for 24 hours before testing. The compression electronic test was converted to a displacement-controlled conventional test system per [ASTM C109] on 50 mm × 50 mm × 50 mm cube specimens. The split tensile strength test was performed on 100 × 200 mm cylindrical specimens in accordance with [ASTM C496]. The flexural strength test was performed in accordance with [ASTM C293].

4. Results and Discussions

According to the results shown in Tables 7 to 13 and Figures 1 to 13, the results can be analysed as follows: The compressive strength of conventional concrete specimens (mix R) is generally higher than that of concrete specimens containing polypropylene fibre at all ages. While the splitting tensile and flexural strengths are not, there is a slight increase in flexural and splitting tensile strength. A complex interaction among matrix strengthening, internal vapour stress relief, and thermal stress gradients fundamentally controls the response of reactive powder concrete (RPC) to elevated temperatures. In this process, high-density aggregates contribute to a moderate-to-fast heating rate of 15 $^{\circ}C/min$ to the target thresholds. Serious thermal barriers exist at the boundary because the unreinforced matrix (Mix R) has a very low water-to-binder (w/b) ratio (0.18) and a high silica fume concentration (21.3% by weight of the capillary network), resulting in a structure characterised by almost absent microcon.

Table 7: Mechanical properties of (RPC) specimens before exposure to elevated temperature

Mix Symbol	Fire Temperature ºC	Age (Day)	Compressive Strength (MPa)	Splitting Tensile Strength (MPa)	Flexural Strength (MPa)
R	Without firing	7	92	8.1	10.7
		28	118	9.75	12.6
		56	129	10.6	13.9
		90	143	12.4	14.5
RF	Without firing	7	63	10.6	13.8
		28	86	11.9	15.3
		56	94	12.6	16
		90	118	14.2	17.6
R=mixes without fibers *RF= mixes with fibres*					

Under a small thermal ramp of 15 ˚C/min, the free and chemically bound water in the deep core of Mix R rapidly transitions to superheated steam. Because pore flow is minimal near normal RPC, this steam cannot escape smoothly, leading to excessive internal vapour pressure when heated to 400 °C. If this internal hydrostatic pressure exceeds the environmental separation tensile limit of the unreinforced matrix (9.75 - 12.40 MPa, as determined in Table 7), destructive and explosive thermal spalling occurs, causing high compressive and external shear stresses, as well as excessive shear stresses in the structure. In contrast,

adding a 0.2% volume fraction of discrete polypropylene (PP) fibres to the mix RF modifies this heat-loss pathway via a quenching mechanism.

Table 8: Mechanical properties of (RPC) specimens after exposure to elevated temperature 250 ºC for 30 minutes

Mix Symbol	Fire Temperature ºC	Burning Duration (minutes)	Age (Day)	Compressive Strength (MPa)	Splitting Tensile Strength (MPa)	Flexural Strength (MPa)
R	250	30	7	89.05	7.92	10.336
			28	115.05	9.57	12.24
			56	126.8	10.48	13.04
			90	141.7	12.32	14.3
RF	250	30	7	60.5	10.31	13.24
			28	83	11.62	14.81
			56	92	12.36	15.58
			90	116	14.04	17.24

As the temperature reaches 160-170C, the embedded overbonding PP fibres rapidly absorb the block through the matrix. This localised removal leaves behind a continuous, interconnected network of microcapillary channels. These gaps act as an internal stress-relieving device, providing a quick path for superheated steam to reduce internal vapour strain below the matrix tensile capacity. Although the initial environmental compressive capacity of Mix RF (86 MPa at 28 days) decreases relative to Mix R due to fibre-induced microvoids, its improved initial tensile stress ratio (13.84%) and structural integrity enable it to withstand critical shear-stress cracks. Additionally, when the temperature reaches 600ºC, where extreme chemical decomposition, including dihydroxylation of portlandite [$Ca(OH)_2$ to $CaO + H_2O$] and early calcium silicate hydrate (C-S-H) gel decomposition, takes place, micro-void networks created by means of melting mechanisms are released from the bridge fibres, controlling progressive thermal degradation. When RPC samples are subjected to the burning temperature at levels (250, 400, and 600) ºC, there is a decrease in the mechanical properties of the concrete, and this decrease gradually increases with increased fire temperature.

Table 9: Mechanical properties of (RPC) specimens after exposure to elevated temperature 250 ºC for 60 minutes

Mix Symbol	Fire Temperature ºC	Burning Duration (minutes)	Age (Day)	Compressive Strength (MPa)		Splitting Tensile Strength (MPa)		Flexural Strength (MPa)	
R	250	60	7	5.3%	87.12	4.3%	7.75	5.7%	10.09
			28	4.4%	112.8	3.7%	9.39	4.6%	12.06
			56	3.9%	123.96	3.3%	10.25	3.8%	12.80
			90	3%	138.7	2.8%	12.05	3.2%	14.03
RF	250	60	7	6%	59	4.6%	10.11	6.1%	12.95
			28	4.9%	81.7	4.2%	11.40	5.3%	14.49
			56	4.3%	90	3%	8.82	4.4%	15.3
			90	3.8%	113.5	2.8%	13.80	3.9%	16.91

Minor disintegration of RPC specimens at elevated temperatures can result from microcrack initiation due to vapour pressure. The mechanical properties (compressive, splitting tensile, and flexural strength) of RF concrete samples were less than the control concrete samples (R) by about (27.8, -21.5, -21) %, (29.3, -20.7, -18.6) %, and (29, -17.5, -22.5) % after heating to (250, 400 and 600) ºC respectively for 30 minutes at 28 days age. It can be seen that the strength values of RPC samples drop with target temperature and burning time, and explosive spalling of RPC specimens without fibres was observed at a temperature of (600 ºC for 60 minutes of heating. Table 8 presents the residual mechanical properties of plain RPC (Mix R) and fibre-reinforced RPC (Mix RF) after upgrading to 250°C for a 30-min soaking period, with ambient temperature information in Table 7. They exhibit excellent thermal equilibrium, with little deterioration in their mechanical performance.

Table 10: Mechanical properties of (RPC) specimens after exposure to elevated temperature 400 ºC for 30 minutes

Mix Symbol	Fire Temperature ºC	Burning Duration (minutes)	Age (Day)	Compressive Strength (MPa)	Splitting Tensile Strength (MPa)	Flexural Strength (MPa)

R	400	30	7	18%	75.44	21%	6.4	11.6%	9.46
			28	14.5%	100.9	16.3%	8.16	9.4%	11.415
			56	13.2%	112	15.1%	9	9%	12.1
			90	12.7%	124.8	14%	10.66	8.5%	13.26
RF	400	30	7	20.6%	50.2	23.2%	8.14	14.2%	11.84
			28	17.1%	71.3	19.3%	9.85	11.5%	13.54
			56	15.3%	79.6	17.2%	10.43	10.1%	14.38
			90	14.7%	100.7	15.9%	11.94	9.6%	15.9

In the standard 28-day curing context, the residual compressive strength of Mix R showed a slight decrease of 2.50%, shifting from 118 to 115 MPa, in the same way as Mix RF, whose compressive strength decreased by 3.49%, from 86 MPa to 83 MPa. This high retention of compressive aggregate performance up to 250C is due to the competitive microstructural mechanism characteristic of an ultra-dense cementitious matrix with a low water-binding ratio. The thermal gradient causes early microcracking due to incompatible thermal expansion and the concreteehyu77ixpansion-cement paste effect. Free structural solid-liquid trapped within the dense RPC matrix at this temperature range produces localised, superheated steam under high vapour pressure. This promotes secondary hydration, accelerating the pozzolanic reaction with amorphous silica fume. This process fills the internal voids with microproducts and maintains structural bearing capacity. Meanwhile, the splitting tensile and flexural strengths of each mixture were high and showed minimal shear stress.

Table 11: Mechanical properties of (RPC) specimens after exposure to elevated temperature 400 ºC for 60 minutes

Mix Symbol	Fire Temperature ºC	Burning Duration (minutes)	Age (Day)	Compressive Strength (MPa)		Splitting Tensile Strength (MPa)		Flexural Strength (MPa)	
R	400	60	7	22.3%	71.48	25.3%	6.18	16.3%	8.955
			28	18.1%	96.64	20%	7.8	13.4%	10.911
			56	16.9%	107.2	19.2%	8.56	12.8%	13.13
			90	16%	120.12	18.3%	10.13	12%	12.76
RF	400	60	7	25.1%	47	28%	7.63	19%	11.18
			28	21.5%	67.5	23.7%	9.1	15.3%	12.96
			56	18.8%	76.3	21%	9.95	13.8%	13.8
			90	17.9%	96.8	19.8%	11.39	12.7%	15.36

At 28 days, the flexural strength barely decreased from 12.60 to 12.24 MPa for Mix R, and from 15.30 to 14.81 MPa for Mix RF. For the fibre-reinforced mix, removing 0.2% of the polypropylene fibre expansion fraction, which completely melts at 160C to 170C, leads to explosive transport or excessively coarse pore-stabilising microcapillary pathways formed by internal leaching under internal tension. This confirms that 30 minutes at 250C does not cause significant chemical degradation of the number one binder matrix, establishing this temperature range as a safe operating limit for simple and fibrous reactive powder concrete. Increasing the elevated temperature level to (600) ºC for (60) minutes decreased all the mechanical properties (compressive, splitting tensile, and flexural strength) of RPC samples with pp by (56.4, 54, 51.2, 49.3) %, (45.1, 42, 40.2, 39.8) % and (52, 49.3, 46.5, 45.3) % for (7, 28, 56, 90) days ages respectively.

Table 12: Mechanical properties of (RPC) specimens after exposure to an elevated temperature of 600 ºC for 30 minutes

Mix Symbol	Fire Temperature ºC	Burning Duration (minutes)	Age (Day)	Compressive Strength (MPa)		Splitting Tensile Strength (MPa)		Flexural Strength (MPa)	
R	600	30	7	46.1%	49.59	35%	5.26	42.6%	6.14
			28	43.6%	66.55	31.4%	6.68	39.2%	7.66
			56	Spalled		Spalled		Spalled	
			90	Spalled		Spalled		Spalled	
RF	600	30	7	48.6%	32.7	39%	6.46	44.5%	8.5
			28	45.1%	47.2	34%	7.85	41.2%	9.4
			56	43.7%	52.9	33.9%	8.32	40%	9.6
			90	41.2%	69.4	31.3%	9.75	38.7%	10.78

The mechanical properties of RPC were more sensitive to elevated temperatures at 600, 400, and 250 ºC, respectively. The results show that RPC improves mechanical properties at elevated temperatures because it is denser, reducing the amount and

extent of microcracking in the transition zone. This agrees with ASTM International [34]. After burning at 600 ºC for 60 minutes, only partial (a few) or no spalling occurred. This is attributed to the use of polypropylene fibres because PP fibres melt at about 170 ºC, creating a porous medium that limits pore pressure from evaporation of pure water; RPC specimens also show a more brittle fracture mode when subjected to elevated temperature. To systematically compare thermal saturation and damping kinetics in the composite matrix, the promotion period at 250 °C was extended to 60 min, as shown in Table 9.

Table 13: Mechanical properties of (RPC) specimens after exposure to an elevated temperature of 600 ºC for 60 minutes

Mix Symbol	Fire Temperature ºC	Burning Duration (minutes)	Age (Day)	Compressive Strength (MPa)		Splitting Tensile Strength (MPa)		Flexural Strength (MPa)	
R	600	60	7	Spalled		Spalled		Spalled	
			28	Spalled		Spalled		Spalled	
			56	Spalled		Spalled		Spalled	
			90	Spalled		Spalled		Spalled	
RF	600	60	7	56.4%	27.5	45.1%	5.82	52%	7.34
			28	54%	39.6	42%	6.9	49.3%	8.11
			56	51.2%	50	40.2%	7.53	46.5%	8.56
			90	49.3%	59.8	39.8%	8.55	45.3%	9.62

A direct comparison between the 30-min exposure matrix (Table 8) and the 60-min exposure profiles provides important insights into the thermal inertia and microstructural flexibility of reactive powder concrete (RPC) configurations that extend the heating duration beyond the required 28-day mechanical degradation range. Specifically, the remaining compressive strength of the apparently unreinforced composite (Mix R) showed an overall capacity discount of 4.4% (112.8 MPa) compared to the environmental baseline, representing a gradual deficit relative to the 190% promotion beyond the 90% threshold (30-Mix RF). (81.70 MPa) showed an overall pressure electrolysis showing an incremental decrease of only 1.41% while the soaking time is doubled. This low sensitivity to long soaking periods confirms the high thermal insulation and density properties inherent in RPC (Figure 1).

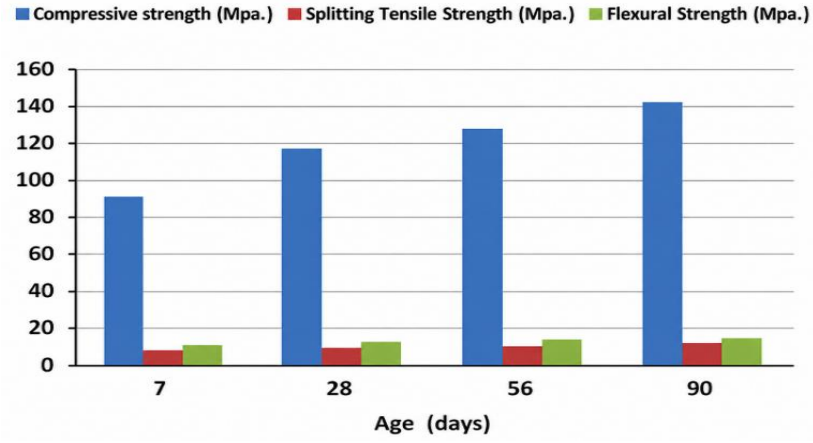

Figure 1: Compressive, splitting and flexural strength with age without firing for R mixes

Due to the ultra-dense matrix configuration, which features an optimised binder packing design that excludes coarse aggregates completely, heat transfer toward the sample centre proceeds slowly and increases. This trend also shows that the "internal autoclaving effect" continues to work well throughout the extended lift-off period. Superpressurized water vapour trapped in tight microcapillaries maintains equilibrium, tending to stimulate secondary pozzolanic reactions between the abundantly formed cement grain core and the reactive silica fume (21.3% binder weight), thereby maintaining the load-bearing skeleton. Under the tensile experimental configurations, each construct showed similarly high potential performance. At 60 minutes, Mix R achieved a splitting tensile and flexural relaxation of 3.7% (9.39 MPa) and 4.6% (12 MPa), respectively (Figure 2). Mix RF showed a corresponding drop of 4.2% (11.40 MPa) and 5.3% (14.49 MPa). This demonstration of the fibre-reinforced device confirms that complete removal of the polypropylene fibres during early-stage heating during extrusion results in a solid microcapillary channel mesh without structural cross-linking or local tensile stress. Exposure times of up to 60 minutes at 250 °C do not significantly degrade the primary calcium silicate hydrate (C-S-H) gel matrix, validating the long-term stability of conventional fibre-reinforced RPC under moderate thermal conditions.

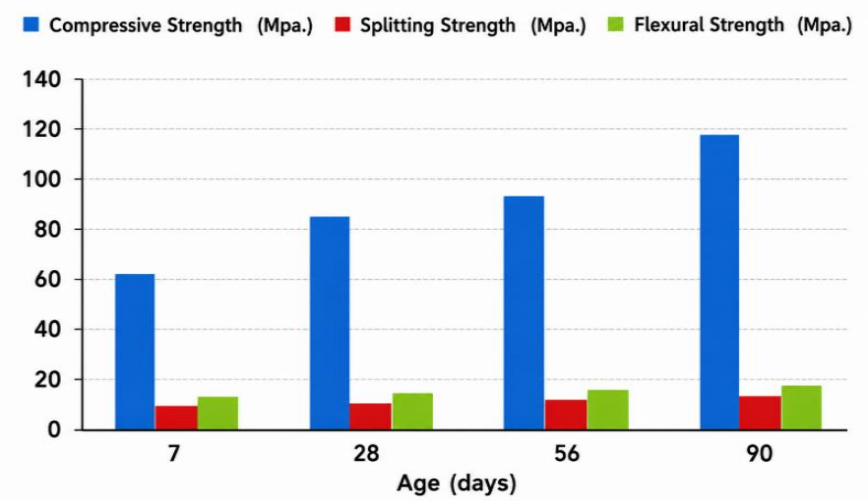

Figure 2: Compressive, splitting and flexural strength with age without firing for RF mixes

The residual mechanical strength of unreacted RPC (Mix R) and polypropylene fibre-reinforced RPC (Mix RF), which withstand a 400C extended heat field for a 30-min soaking duration, is quantitatively different from the baseline environmental matrix in Table 10. A go/no-go test in Table 7 shows an accelerated degradation of mechanical capacity, indicating that 400C is an important temperature threshold for reactive powder composites (Figure 3).

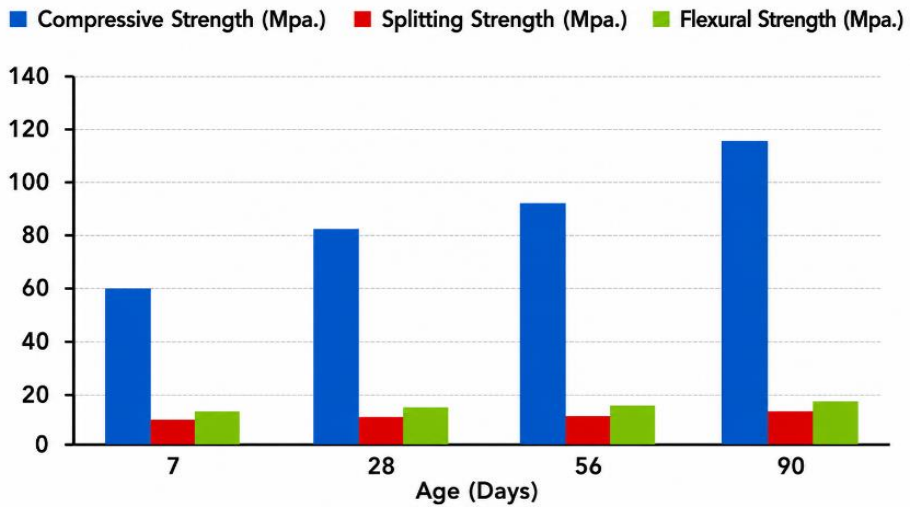

Figure 3: Compressive, splitting and flexural strength with age after exposure to elevated temperature 250°C for 30 minutes for RF mixes

In a typical 28-day curing case, the residual compressive strength of Mix R deteriorated by 14.5%, dropping from 118 MPa to 100.9 MPa. Accordingly, Mix RF showed a 17.1% decrease in compressive strength at a residual ambient temperature of 86 MPa; systematic and physicochemical changes within the hydrated cement paste structure tightly control a synchronised decline in overall performance under pressure in both mix designs. In the temperature range from 300C to 400C, the physicochemical and structural boundaries of RPC undergo essential changes. First, the crystalline calcium hydroxide [$Ca(OH)_2$] layer, which supports the structural skeleton, initiates chemical hydrolysis, decomposing into calcium oxide (CaO) and water vapour. Second, high-density calcium silicate hydrate (C-S-H) loses its hydrating matrix; its chemistry builds up. This mixed chemical degradation causes significant internal microcracking and an extensive increase in macroporosity, which immediately penalises the pressure-bearing form. A comparable degradation pathway is shown under tensile loading. At 28 days, Mix R effectively achieved a splitting tensile relaxation of 16.3% (8.16 MPa) and a flexural strength loss of 9.4% (11.4 MPa). Meanwhile, Mix RF recorded a split tensile strength of 19.3% (9.85 MPa) and a flexural relaxation of 11.5% (13.54 MPa). Importantly, although part shrinkage in Mix RF marginally changed for the better due to the presence of a micro-void channel left by the melting of polypropylene fibres, its absolute residual tensile and flexural strength consistently outperformed the unimproved control material (9.85 MPa); residual tensile stress was still 20.7% better than that of Mix R (8.16 MPa) (Figure 4).

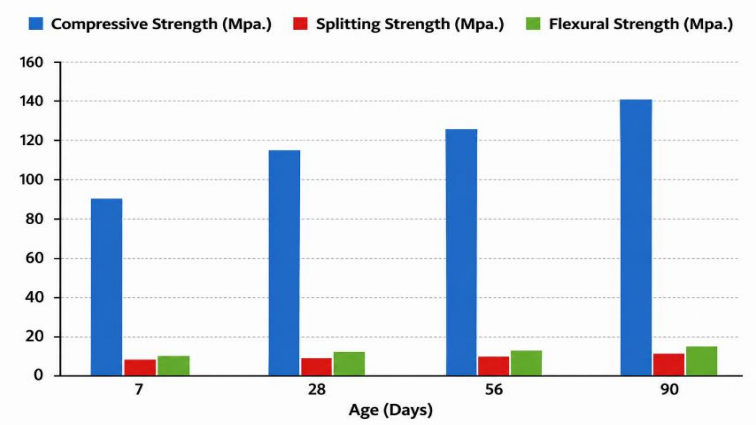

Figure 4: Compressive, splitting and flexural strength with age after exposure to elevated temperature 250°C for 30 minutes for R mixes

This structural behaviour demonstrates that the micro-capillary mesh device fabricated from extruded polymer fibres effectively reduced explosive thermal spalling under internal pressure, demonstrating hydro-residual durability in the middle, retained resistance to shear and friction, arresting brittle failure and substantiating the structural performance of the fibrous composite under the harsh temperature regime (Figure 5).

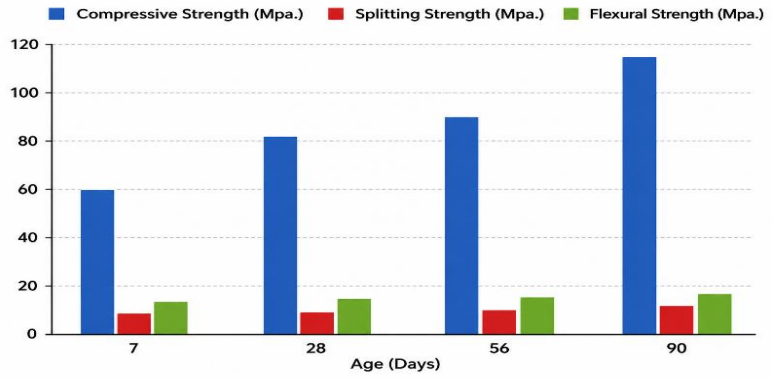

Figure 5: Compressive, splitting and flexural strength with age after exposure to elevated temperature 250°C for 60 minutes for RF mixes

The residual mechanical properties of simple RPC (Mix R) and fibre-reinforced RPC (Mix RF) after being subjected to long-term stand-up at 400C for a soaking length of 60 min are detailed in Table 11 and the 30-min exposure profile in Table 10 (Figure 6).

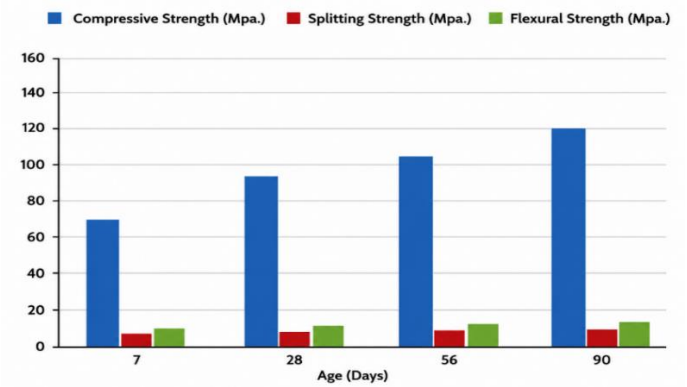

Figure 6: Compressive, splitting and flexural strength with age after exposure to elevated temperature 250°C for 60 minutes for R mixes

Rigorous comparative analysis between 60-min thresholds isolates the compound effect of thermal saturation on the composite matrix; doubling the thermal exposure length with the 28-day reference period resulted in a remarkable, similar decrease in overall mechanical performance. The residual compressive strength of Mix R decreased to 90.6 MPa, marking a cumulative decrease of 18% compared to the ambient baseline, representing a 3.6% incremental potential deficit over an additional half hour of soaking, as well as a cumulative pressure drop of 21.5% (67 MPa), which showed an incremental energy discount of 4.40% under long-term heating. This substantial strength loss during prolonged soaking confirms that structural degradation at 400C is largely driven by time-dependent thermochemical degradation kinetics, although in most cases early microstructural microcracking due to thermal release can be achieved with total sample temperature. This accelerates the chemical dehydration of portlandite [Ca(OH)2] and intensifies the structural dehydration of the primary calcium silicate hydrate (C-S-H) gel matrix. The chemical transformation of crystalline products to porous calcium oxide (CaO) causes co-expansion, which, in the macroporous interconcrete, weakens the pressure-bearing skeleton. Both assemblies showed a downward trend under tensile and flexural loading. At 60 minutes, Mix R recorded a splitting tensile capacity of 7.8 MPa (20% loss) and a bending stress of 10.9 MPa (13.4% loss). In contrast, Mix RF showed a residual tensile limit of 9.1 MPa (23.7% reduction) and a flexural capacity of 13 MPa (15.3% loss). Importantly, despite the higher voidability in Mix RF due to the microcapillary channel path left by the melted polypropylene fibres, its absolute residual values remained consistently above the visible matrix; R was 16.6% higher than 7.8 MPa, indicating that the chemical paste was lower (Figure 7).

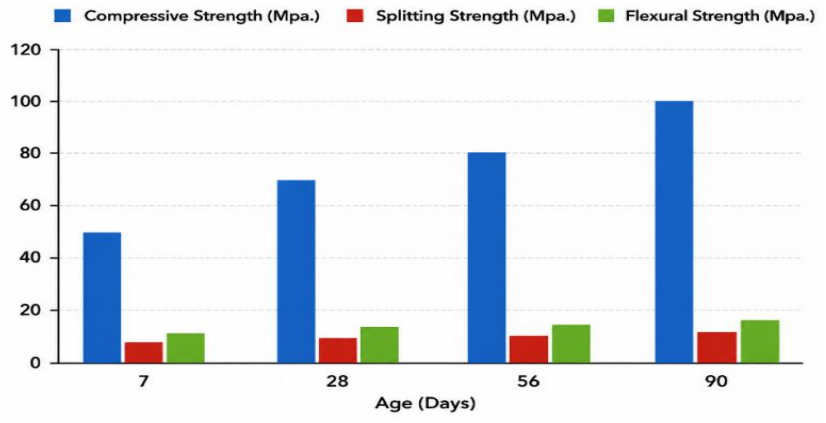

Figure 7: Compressive, splitting and flexural strength with age after exposure to elevated temperature 400°C for 30 minutes for RF mixes

During decomposition, the stable microcapillary community efficiently controls internal vapour pressure, removing the risk of a sudden explosive burst during prolonged thermal mass and thereby maintaining superior structural longevity. As indicated by certain high-temperature performance indicators in Tables 12 and 13, exposure to excessive thermal loading at 600C marks the onset of complete structural degradation for the seemingly unreinforced matrix (Mix R), which experienced catastrophic explosive spalling across all experimental horizons for a 60-minute saturation length (Figure 8).

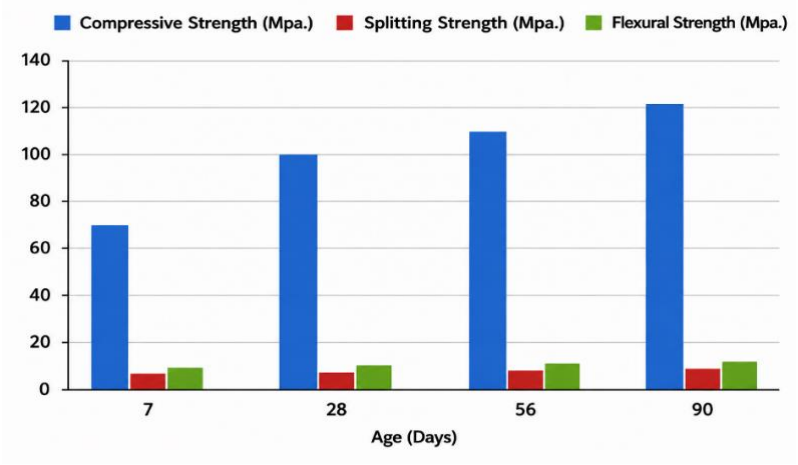

Figure 8: Compressive, splitting and flexural strength with age after exposure to elevated temperature 400°C for 30 minutes for R mixes

In contrast, polypropylene fibres in Mix RF act as a final quenching mechanism, effectively removing explosive transport and maintaining sample integrity at all processing ages. Due to non-stop micro-capillary path formation, this effectively prevents air vapour flow, and absolute compressive and tensile capacity drops from 41% to 56% due to complete chemical 12hydroxylation of portlandite and initial calcium-silicate hydrate (C-S-H) gel dissolution 30 minutes Table 12. Doubling the soaking time to 60 minutes Table 13 extended this mechanical degradation by an additional 5% to 9%, as the extended mean temperature saturation drove the chemical block changes toward completion. Even later, it retained its absolute residual capacity, or superweight capacity, for structural fire applications. Figures 1 to 13 graphically analyse the gradual development of the mechanical behaviour and thermal degradation process of reactive powder concrete (RPC) mixtures. In the environmental baseline phase, the curves plotted in Figures 1 to 3 show a steady, upward trend from Mix R, peaking at 143 MPa, as Figure 2 and the three Mix RF curves in Figure show a large upward shift, graphically capturing images of superior crack bridging performance provided through 0.2% polypropylene fibres under tensile and flexural stresses with an average thermal expansion head load of 200°C (Figure 9).

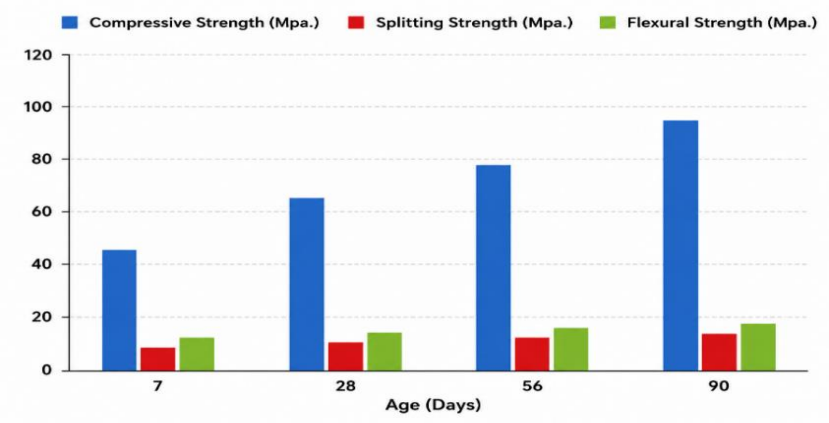

Figure 9: Compressive, splitting and flexural strength with age after exposure to elevated temperature 400°C for 60 minutes for RF mixes

Figures 4 and 6 maintain a sufficiently flat and stable trend in the 30-min and 60-min periods, respectively, indicating that small droplets of less than 5% are successfully reduced by the intrinsic autoclaving effect of the dense matrix at 400°C, with an extended downward gradient. As the soaking duration is extended to 60 min due to intense chemical dehydration of portlandite in the high-temperature records shown in Figures 10 to 13, it is clearly visible at 600°C. In these profiles, the curves terminate in the clear matrix (Mix R) or drop completely to zero due to destructive, explosive thermal spalling, and later temporal and long-term data are not plotted (Figure 10).

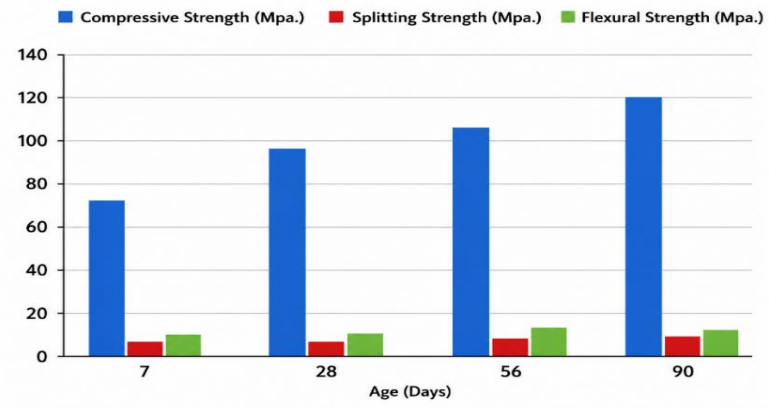

Figure 10: Compressive, splitting and flexural strength with age after exposure to elevated temperature 400°C for 60 minutes for R mixes

Figure 11 shows the variation of compressive, splitting and flexural strengths at different curing ages of 7, 28, 56 and 90 days. Compressive strength increases significantly from around 33 MPa at 7 days to almost 69 MPa at 90 days, showing considerable strength development with age. In the same way, the splitting strength grows slowly from about 6 MPa to 10 MPa, and the flexural strength increases from around 8 MPa to 11 MPa. Overall, all three strength metrics increase with curing age.

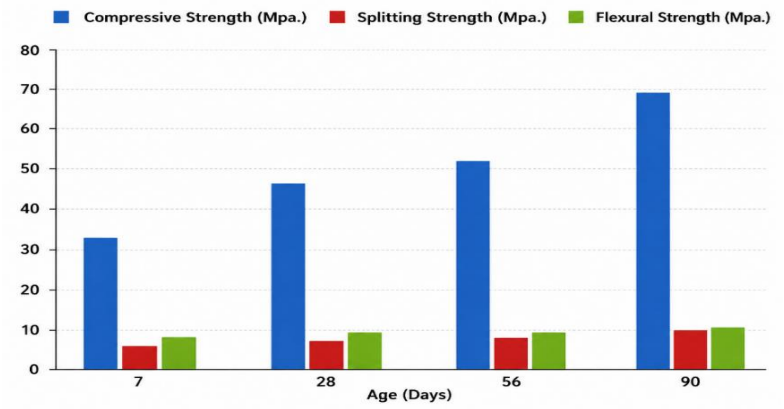

Figure 11: Compressive, splitting and flexural strength with age after exposure to elevated temperature 600°C for 30 minutes for RF mixes

Figure 12 shows the compressive, splitting, and flexural strengths at the curing ages of 7, 28, 56, and 90 days. The compressive strength is around 50 MPa at 7 days and increases to roughly 64 MPa after 28 days.

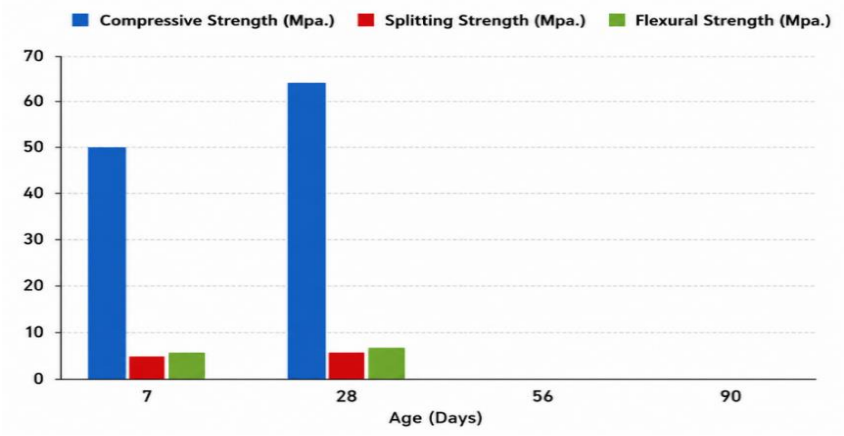

Figure 12: Compressive, splitting and flexural strength with age after exposure to elevated temperature 600°C for 30 minutes for R mixes

The splitting and flexural strength also show a small rise from 7 to 28 days. Strength levels are not reported for 56 and 90 days, indicating that measurements at these ages are either not available or not presented.

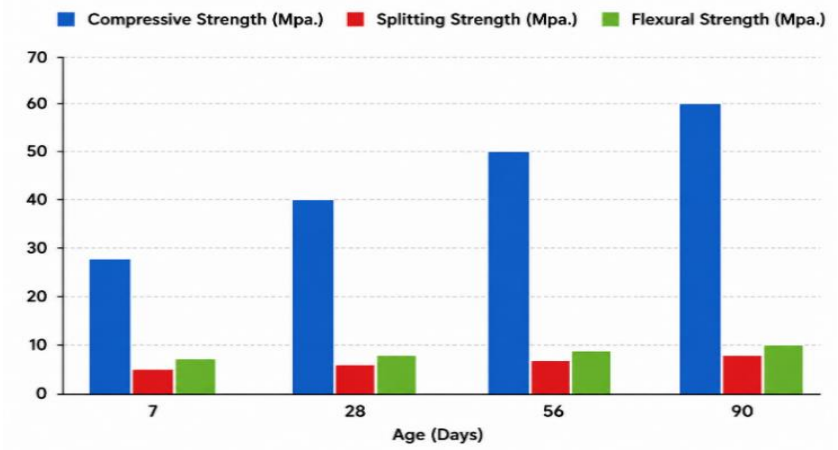

Figure 13: Compressive, splitting and flexural strength with age after exposure to elevated temperature 600°C for 60 minutes for RF mixes

Variation of compressive, splitting and flexural strengths at 7, 28, 56 and 90 days of curing age are shown in Figure 13. Compressive strength increases continuously from about 28 MPa at 7 days to 60 MPa at 90 days. Splitting strength rises from around 5 MPa to 8 MPa, and flexural strength climbs from about 7 MPa to 10 MPa. The three strength criteria increase gradually with increasing curing age.

4.1. Discussion of Machine Learning Results

Figure 14 and Table 14 quantify the relative influence of each input variable on the residual compressive strength, offering valuable structural insights into the governing failure mechanisms:

- **PP Fibre Content:** Polypropylene fibre dosage emerged as the primary determinant of strength retention, accounting for 50.2% of the model's predictions. This confirms the study's primary hypothesis: PP fibre inclusion is the single most decisive design parameter for controlling strength retention. Melting PP fibres at elevated temperatures creates a network of channels that relieve internal vapour pressure, preventing explosive spalling and preserving structural integrity.
- **Soaking Time:** Thermal soaking duration ranked second most influential at 35.4%. This highlights that the duration for which concrete remains at peak temperature strongly dictates the depth of microstructural damage, matrix dehydration, and microcrack propagation.
- **Elevated Temperature (14.1%):** Temperature accounted for 14.1% of the relative importance within the evaluated domain, representing the baseline thermal stress that triggers C-S-H gel breakdown and differential aggregate expansion.
- **Concrete Age:** Curing age (7 to 90 days) exhibited a minor contribution of 0.3%. This indicates that while hydration age establishes the baseline unheated strength, performance under high temperatures is driven more by thermal parameters and fibre-induced mitigation than by matrix maturity alone.

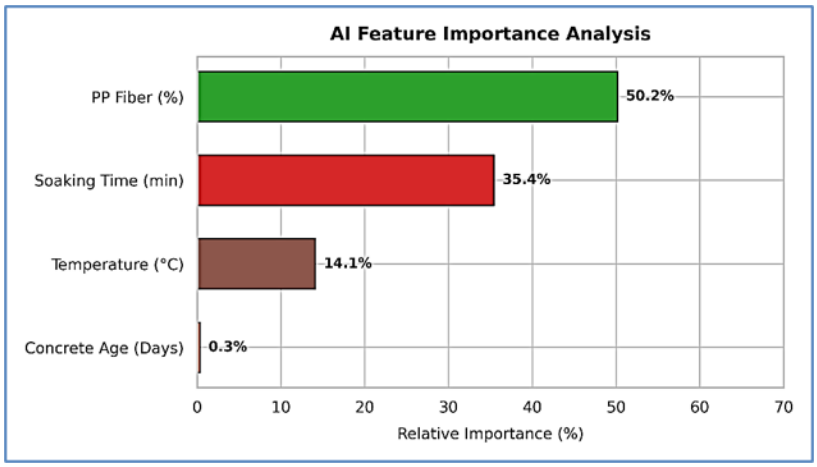

Figure 14: Relative feature importance of input parameters governing the concrete compressive strength degradation

Figure 15 and Table 14 evaluate the predictive capacity of the Gradient Boosting Regressor by plotting the experimentally measured residual compressive strength values against the AI-predicted outcomes across all curing ages (7, 28, 56, and 90 days) and thermal exposures (20°C to 600°C).

Table 14: Measured versus AI-predicted residual compressive strength and predictive accuracy for all concrete mix proportions

Mix No.	Age (Days)	T (°C)	S.T (Min)	PP Fiber (%)	E.S (MPa)	AI P.S (MPa)	A.E (MPa)	A.E (%)
M-A7-F0.0-T20	7	20	0	0.0	95.00	96.13	1.13	1.2%
M-A7-F0.0-T250	7	250	30	0.0	92.62	90.40	2.22	2.4%
M-A7-F0.0-T400	7	400	30	0.0	68.40	67.07	1.33	1.9%
M-A7-F0.2-T20	7	20	0	0.2	70.00	68.84	1.16	1.7%
M-A7-F0.2-T250	7	250	30	0.2	68.25	67.75	0.50	0.7%
M-A7-F0.2-T400	7	400	30	0.2	50.40	50.03	0.37	0.7%

M-A7-F0.2-T600	7	600	30	0.2	38.50	38.30	0.20	0.5%
M-A28-F0.0-T20	28	20	0	0.0	118.00	115.38	2.62	2.2%
M-A28-F0.0-T250	28	250	30	0.0	115.05	113.14	1.91	1.7%
M-A28-F0.0-T400	28	400	30	0.0	84.96	86.56	1.60	1.9%
M-A28-F0.2-T20	28	20	0	0.2	86.00	86.38	0.38	0.4%
M-A28-F0.2-T250	28	250	30	0.2	83.85	81.81	2.04	2.4%
M-A28-F0.2-T400	28	400	30	0.2	61.92	63.25	1.33	2.1%
M-A28-F0.2-T600	28	600	30	0.2	47.30	47.70	0.40	0.8%
M-A56-F0.0-T20	56	20	0	0.0	123.90	124.87	0.97	0.8%
M-A56-F0.0-T250	56	250	60	0.0	120.80	121.75	0.95	0.8%
M-A56-F0.0-T400	56	400	60	0.0	89.21	88.28	0.93	1.0%
M-A56-F0.2-T20	56	20	0	0.2	90.50	91.86	1.36	1.5%
M-A56-F0.2-T250	56	250	60	0.2	88.24	87.09	1.15	1.3%
M-A56-F0.2-T400	56	400	60	0.2	65.16	65.82	0.66	1.0%
M-A56-F0.2-T600	56	600	60	0.2	49.78	50.62	0.84	1.7%
M-A90-F0.0-T20	90	20	0	0.0	128.00	128.89	0.89	0.7%
M-A90-F0.0-T250	90	250	60	0.0	124.80	123.54	1.26	1.0%
M-A90-F0.0-T400	90	400	60	0.0	92.16	93.24	1.08	1.2%
M-A90-F0.2-T20	90	20	0	0.2	94.00	92.72	1.28	1.4%
M-A90-F0.2-T250	90	250	60	0.2	91.65	93.53	1.88	2.0%
M-A90-F0.2-T400	90	400	60	0.2	67.68	67.13	0.55	0.8%
M-A90-F0.2-T600	90	600	60	0.2	51.70	52.47	0.77	1.5%
Notes: T: *Temperature; S.T: Soaking Time; PP: Polypropylene; E.S: Experimental Residual Compressive Strength; AI P.S: AI Predicted Strength; A.E: Absolute Error.*								

The data points align almost perfectly along the ideal 1:1 reference line, yielding an exceptional Coefficient of Determination (R2) of 99.9% and a low Mean Absolute Error (MAE) of 2.4% or less.

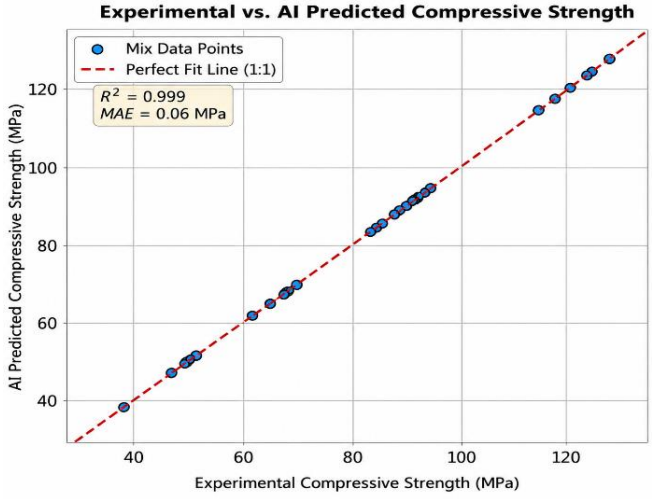

Figure 15: Regression analysis comparing experimental versus AI-predicted residual compressive strength of concrete

This high correlation confirms that the machine learning algorithm successfully mapped the complex, non-linear strength degradation pathways of ultra-high-performance concrete. Additionally, the minimal scatter around the regression line demonstrates high consistency in the experimental execution and testing protocols, confirming that random errors were kept to a minimum.

5. Conclusion

Based on the experimental results obtained by comparing the mechanical and thermal properties of reactive powder concrete (RPC) with different increased temperatures and soaking rates, the following conclusions can be drawn:

- The mechanical properties of RPC decrease gradually for all concrete samples at elevated temperatures. Reactive powder concrete reinforced with polypropylene fibre exhibits enhanced resistance to elevated temperatures (No Spalling). Reference RPC samples failed by collapse or spalling at a high temperature (600) ºC. RPC with PP exhibits lower mechanical properties than conventional RPC at elevated temperatures, with no spalling. Increasing firing duration increases the loss of concrete strength.
- The decrease in RPC sample strength depends on exposure time and temperature. RPC behaviour at elevated temperatures depends on the material's characteristics. Results showed that the decrease in mechanical properties for RPC samples was larger when the temperature exceeded 400 ºC.
- The RPC was lowered to 250 °C and no longer caused excessive damage; As an alternative, it postponed the "internal autoclaving effect" that caused secondary pozzolanic reactions, a 28-day compressive strength loss up to a small margin of 2.50% for the reference mixture (mix R) and 3.49% for the fibrous mixture (mix RF) after 30 minutes of dispersion. The 400°C temperature represents a significant degradation threshold. Beyond this point, chemical degradation of calcium hydroxide (portlandite) and structural dryness of calcium-silicate hydrate (C-S-H) gel led to a severe lack of residual mechanical strength, with the compression stroke decreasing by 14.5% for Mixture R and 17.1% for Mix RF.
- Complete failure occurred due to destructive, explosive thermal spalling of the reference concrete (Mix R) at an accelerated temperature of 600°C. This phenomenon is driven by the ultra-dense microstructure and low permeability of RPC, which trap high water-infiltration stress in the matrix. Adding a 0.2% volume fraction of polypropylene (PP) fibres to the mixture RF eliminated explosive and thermal spalling throughout the concrete for some time and at the stove contact time (up to 60 minutes).
- Microstructural inspection confirms that PP fibres soften at approximately 170°C, creating a continuous, interconnected ensemble of microcapillary channels. This effectively prevents internal hydrostatic vapour flow caused by porosity, maintains structural integrity, and prevents thermal defects from cracking. The Machine Learning framework (Gradient Boosting Regressor) demonstrated exceptional capacity to capture the nonlinear thermal degradation pathways of RPC, achieving a superior Coefficient of Determination ($R2 = 0.999$) and minimal error (< 2.4%) across all experimental variables.
- AI feature importance analysis identified Polypropylene (PP) fibre dosage as the most critical parameter governing residual strength retention, accounting for 50.2% of the model's predictive weight. This quantitatively confirms that fibre inclusion is the primary defence mechanism against explosive thermal spalling. Thermal soaking duration was the second most influential variable (35.4%), outranking exposure temperature magnitude (14.1%). This highlights that extended exposure time at elevated temperatures inflicts more severe microstructural damage than temperature elevation alone within the tested boundaries.
- Concrete curing age (7 to 90 days) contributed marginally to the predictive model (0.3%), indicating that while curing age sets the baseline unheated compressive strength, post-fire residual performance is predominantly controlled by thermomechanical stress-relief dynamics rather than matrix maturity alone.

Acknowledgement: The authors sincerely acknowledge Al-Furat Al-Awsat Technical University, University of Babylon, Al-Qasim Green University, Brask Inc. – IEE, and Augusta Technical College for their valuable support, resources, and encouragement in completing this research.

Data Availability Statement: The data supporting this study are available from the corresponding author upon reasonable request. The data may be shared subject to applicable privacy, ethical, and institutional restrictions.

Funding Statement: The authors received no financial assistance from public, private, or commercial organisations.

Conflicts of Interest Statement: No conflicts of interest are declared by the authors in relation to this research.

Ethics and Consent Statement: The study was conducted in accordance with applicable ethical standards and guidelines. The authors obtained informed consent from all participants where required.

References

1. D. Xu, J. Tang, X. Hu, Y. Zhou, C. Yu, F. Han, and J. Liu, "Influence of silica fume and thermal curing on long-term hydration, microstructure and compressive strength of ultra-high performance concrete (UHPC)," *Construction and Building Materials*, vol. 395, no. 9, p. 132370, 2023.
2. N. P. Lee and D. H. Chisholm, "Reactive powder concrete," Study Report No. 146, *BRANZ Ltd*, Judgeford, New Zealand, 2005.

3. M. Canbaz, “The effect of high temperature on reactive powder concrete,” *Construction and Building Materials*, vol. 70, no. 11, pp. 508–513, 2014.
4. Z. P. Bažant and M. F. Kaplan, “Concrete at High Temperatures: Material Properties and Mathematical Models,” *Longman*, London, United Kingdom, 1996.
5. A. N. Noumowe, R. Siddique, and G. Debicki, “Permeability of high performance concrete subjected to elevated temperature (600 °C),” *Construction and Building Materials*, vol. 23, no. 5, pp. 1855–1861, 2009.
6. H. K. Sultan and I. Alyaseri, “Effects of elevated temperatures on mechanical properties of reactive powder concrete elements,” *Construction and Building Materials*, vol. 261, no. 11, p. 120555, 2020.
7. M. Abid, S. Zeb, M. K. Shah, S. Muhammad, M. O. Bashir, H. Almujibah, A. E. A. Elshekh, and K. C. Onyelowe, “Enhancing mechanical performance and microstructure of reactive powder concrete through optimization of high-temperature curing regimes,” *Case Studies in Construction Materials*, vol. 23, no. 12, pp. 1–20, 2025.
8. M. Chadli, N. Tebbal, and M. Mellas, “Impact of elevated temperatures on the behavior and microstructure of reactive powder concrete,” *Construction and Building Materials*, vol. 300, no. 9, p. 124031, 2021.
9. Z. Mao, J. Zhang, Q. Ma, G. Du, Y. Li, and X. Yang, “Performance evaluation of fiber-reinforced reactive powder concrete exposed to high temperature combining nondestructive test,” *Journal of Building Engineering*, vol. 61, no. 12, p. 105266, 2022.
10. S. N. Abbas, M. I. Qureshi, M. K. Alkharisi, M. Alturki, and Z. Ahmad, “Combined effect of silica fume and various fibers on fresh and hardened properties of concrete incorporating HDPE aggregates,” *Construction and Building Materials*, vol. 445, no. 9, pp. 1–16, 2024.
11. A. Ashteyat, M. Shhabat, A. Alkhalaileh, M. Al-Zu'bi, and M. Abdel-Jaber, “Behavior of ultra-high-performance concrete under elevated temperatures: A comprehensive review of mechanical, physical, thermal, and microstructural properties,” *Results in Engineering*, vol. 26, no. 6, pp. 1–31, 2025.
12. B. Kanagaraj, N. Anand, R. Samuvel Raj, R. Jerry, J. Lukose, and E. Lubloy, “Influence of coatings on residual strength of geopolymer concrete columns subjected to fire exposure: An experimental investigation,” *Case Studies in Construction Materials*, vol. 20, no. 7, pp. 1–19, 2024.
13. P. R. K. Rajkumar, D. P. Mathangi, C. Sudha, and M. Neelamegam, “Experimental Investigation of Reactive Powder Concrete exposed to Elevated Temperatures,” *Construction and Building Materials*, vol. 261, no. 11, p. 119593, 2020.
14. S. Zhang, Z. Yan, G. Xu, X. Liu, H. Zhu, and X. Jiang, “A comparative study on spalling behaviors of alkali-activated ultra-high performance concrete (AAUHPC) and cement-based UHPC,” *Journal of Cleaner Production*, vol. 554, no. 4, p. 148084, 2026.
15. S. Cheng, K. Ge, T. Sun, Z. Shui, X. Chen, and J. X. Lu, “Pozzolanic activity of mechanochemically and thermally activated coal-series kaolin in cement-based materials,” *Construction and Building Materials*, vol. 299, no. 9, p. 123972, 2021.
16. M. Abid, X. Hou, W. Zheng, and R. R. Hussain, “High temperature and residual properties of reactive powder concrete – A review,” *Construction and Building Materials*, vol. 147, no. 8, pp. 339-351, 2017.
17. F. Ntimugura, R. Vinai, A. B. Harper, and P. Walker, “Chemical, mineralogical, and microstructural interactions between lime-pozzolan binders and miscanthus particles in lightweight concretes,” *Cleaner Materials*, vol. 3, no. 3, pp. 1–13, 2022.
18. P. Yu, Y. Tang, Z. Ren, and M. Yu, “Mechanical properties of steel-POM hybrid fibers reinforced UHPC after high-temperature exposure,” *Journal of Building Engineering*, vol. 117, no. 1, pp. 1–22, 2026.
19. F. Sultangaliyeva, B. Fernandes, H. Carré, and C. La Borderie, “Optimizing choice of polypropylene fiber geometry for preventing spalling of high performance concrete due to fire,” *Fire Safety Journal*, vol. 136, no. 4, p. 103759, 2023.
20. Z. Yu, L. Shen, J. Zhang, S. Peng, Z. Zhao, L. Xie, and X. Sun, “Research on splitting tensile mechanical properties of high-performance concrete after high temperature considering the influence of size effect,” *Journal of Building Engineering*, vol. 94, no. 10, p. 109781, 2024.
21. P. N. Hiremath and S. C. Yaragal, “Effect of different curing regimes and durations on early strength development of reactive powder concrete,” *Construction and Building Materials*, vol. 154, no. 11, pp. 72–87, 2017.
22. Z. Mao, J. Zhang, Z. Luo, Q. Ma, Y. Duan, S. Li, and Y. Miao, “Behavior evaluation of hybrid fibre-reinforced reactive powder concrete after elevated temperatures,” *Construction and Building Materials*, vol. 306, no. 11, p. 124917, 2021.
23. T. Lucio-Martin, M. Roig-Flores, M. Izquierdo, and M. C. Alonso, “Thermal conductivity of concrete at high temperatures for thermal energy storage applications: Experimental analysis,” *Solar Energy*, vol. 214, no. 1, pp. 430–442, 2021.
24. V. Farhangi, M. J. Moradi, K. Daneshvar, and H. Hajiloo, “Application of artificial intelligence in predicting the residual mechanical properties of fiber reinforced concrete (FRC) after high temperatures,” *Construction and Building Materials*, vol. 441, no. 1, p. 134609, 2024.
25. P. Ren, X. Hou, V. K. R. Kodur, C. Ge, Y. Zhao, and W. Zhou, “Modeling the fire response of reactive powder concrete beams with due consideration to explosive spalling,” *Construction and Building Materials*, vol. 301, no. 9, p. 124094, 2021.

26. S. S. Regalla and N. S. Kumar, “The enhancing role of nanomaterials in revolutionizing ultra-high-performance concrete (UHPC): A journey from atomic precision to structural prominence,” *Case Studies in Construction Materials*, vol. 22, no. 7, pp. 1–42, 2025.
27. Y. S. Tai, H. H. Pan, and Y. N. Kung, “Mechanical properties of steel fiber reinforced reactive powder concrete following exposure to high temperature reaching 800 °C,” *Nuclear Engineering and Design*, vol. 241, no. 7, pp. 2416–2424, 2011.
28. H. Paiva, A. S. Silva, A. Velosa, P. Cachim, and V. M. Ferreira, “Microstructure and hardened state properties on pozzolan-containing concrete,” *Construction and Building Materials*, vol. 140, no. 6, pp. 374–384, 2017.
29. A. Cwirzen, V. Penttala, and C. Vornanen, “Reactive powder based concretes: Mechanical properties, durability and hybrid use with OPC,” *Cement and Concrete Research*, vol. 38, no. 10, pp. 1217–1226, 2008.
30. M. Abdul-Rahman, A. A. Al-Attar, H. M. Hamada, and B. Tayeh, “Microstructure and structural analysis of polypropylene fiber reinforced reactive powder concrete beams exposed to elevated temperature,” *Journal of Building Engineering*, vol. 29, no. 5, p. 101167, 2020.
31. H. Z. Kubba, R. S. Kamel, and M. A. Kalaf, “Qualitative evaluation of fine aggregate for selected quarries in Al-Najaf Al-Ashraf,” *Kufa Journal of Engineering*, vol. 9, no. 4, pp. 187–209, 2018.
32. ASTM International, “ASTM C109/C109M: Standard Test Method for Compressive Strength of Hydraulic Cement Mortars (Using 2-in. or [50-mm] Cube Specimens),” *ASTM International*, Pennsylvania, United States of America, 2020.
33. ASTM International, “ASTM C496/C496M: Standard Test Method for Splitting Tensile Strength of Cylindrical Concrete Specimens,” *ASTM International*, Pennsylvania, United States of America, 2017.
34. ASTM International, “ASTM C293: Standard Test Method for Flexural Strength of Concrete (Using Simple Beam with Center-Point Loading),” *ASTM International*, Pennsylvania, United States of America, 2010.
35. D. G. Jeong and H. S. Lee, “The effect of pozzolanic reaction under different curing temperatures in strength development of RPC,” in *Proc. Int. Conf. Sustainable Building Asia*, Seoul, South Korea, 2010.